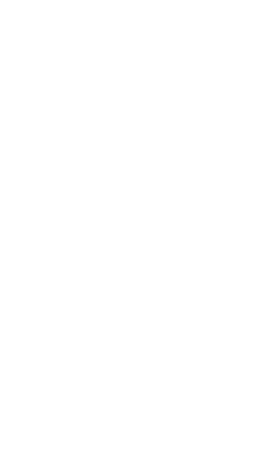



[All Posts](#)


Lior Ella

Jump to:

- [Introduction](#)
- [Qubit Initialization Implementation](#)
- [Active Reset Results](#)
- [References](#)

How to Dramatically Increase the Initialization Fidelity of Your Qubits with QUA

October 25 | 2021



Introduction

Qubit initialization is crucial for useful quantum computing, and there are various methods in which it is implemented. Whenever we see circuits showing various algorithms, we take it as given that the qubits all start out in their ground state. However, in reality, we cannot take this for granted. Qubit reset, a technique used to bring the qubits to their ground state, can be implemented using various methods. The simplest and least demanding method for qubit reset, or qubit state initialization, is to wait for the qubits to decay to their thermal state. While this is indeed a possibility, it suffers from several drawbacks. Firstly, it's very time costly, as you need to wait for the qubits to fall back to their ground state. In fact, as qubit lifetimes steadily improve, this time is expected to grow prohibitively long and become a major bottleneck for achieving high throughput quantum circuits. Secondly, there's always spontaneous excitation that occurs; there's always a chance that the qubit is not actually in the ground state, thus causing the preparation fidelity to be limited by the thermal distribution of the qubit states.

Active reset tackles both of these problems. It 1) reduces the qubit initialization time, and 2) improves the probability that the qubit is indeed in the ground state after the initialization. Here we will show you how a 3-way collaboration between Q-CTRL, using their *Boulder Opal*, the Delft lab at LNL and Quantum Machines' *Quantum Orchestration Platform*, allows you to perform highly efficient qubit reset protocols with state machine logic that is cleverly optimized for superconducting qubits. If you want to implement similar Q-CTRL protocols with QUA, please refer to the how-to guide for integrating Q-CTRL's *Boulder Opal* with QUA, and the *Q-CTRL python add-on package* for QUA.

There are several figures of merit which need to be considered when examining various initialization schemes. Specifically, we assess the quality of initialization by measuring two parameters: the ground state preparation probability and the time required to reach that probability. We can thus plot various initialization schemes, where the x-axis is the preparation time, and the y-axis is the preparation success probability. The closer the curve to the top left (low preparation time, high success probability), the better. An example of such a family of curves can be seen in Figure 1.

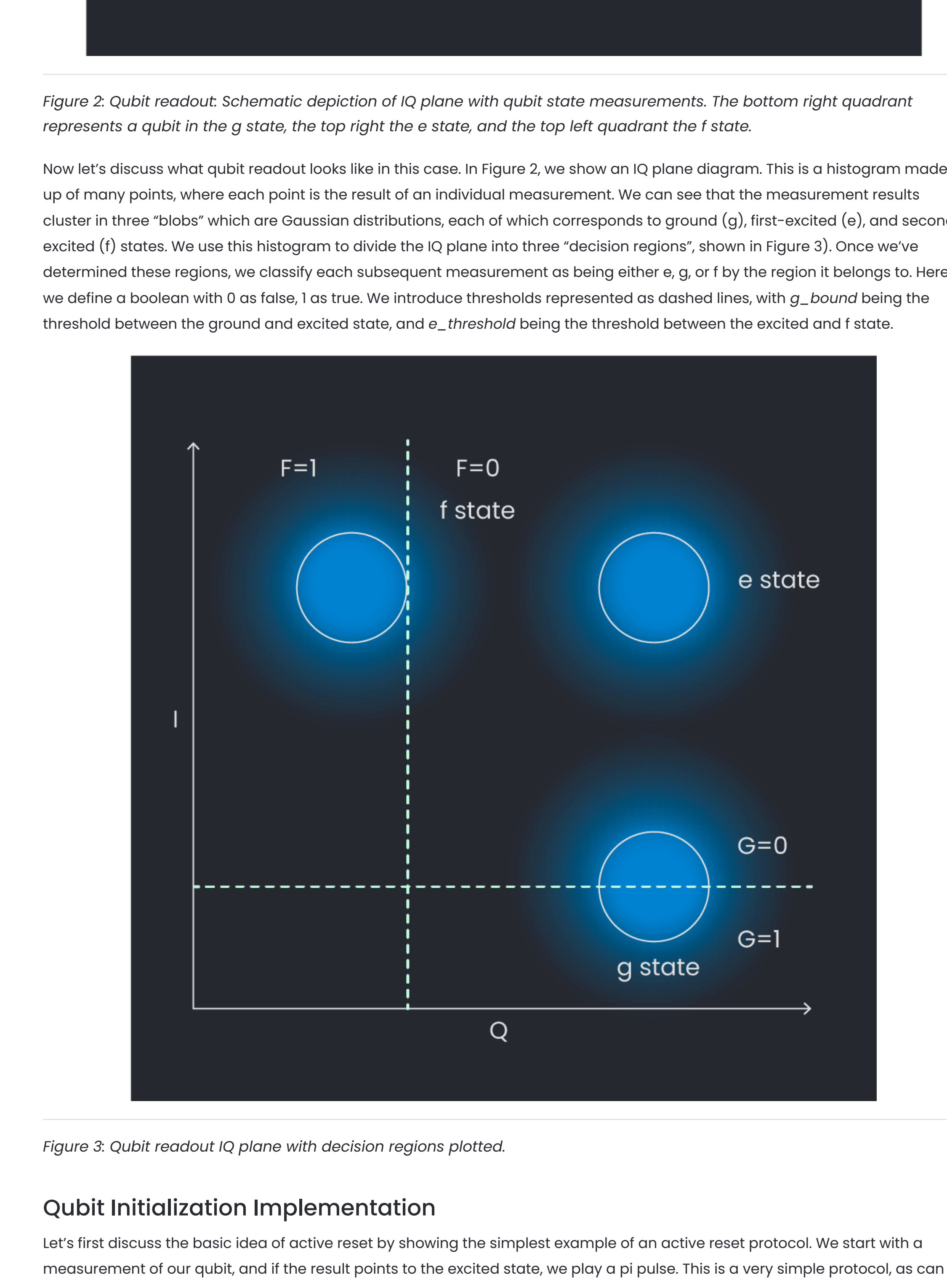


Figure 1: Schematic depiction of fidelity over time for various initialization schemes. The red line represents an initialization scheme that cannot, in principle, reach unit fidelity. The blue and green schemes can both reach unit fidelity, but the green one will achieve a given fidelity for a shorter initialization time than the blue and is therefore superior to it.



Figure 2: Qubit readout: Schematic depiction of IQ plane with qubit state measurements. The bottom right quadrant represents a qubit in the g state, the top right the e state, and the top left quadrant the f state.

Now let's discuss what qubit readout looks like in this case. In Figure 2, we show an IQ plane diagram. This is a histogram made up of many points, where each point is the result of an individual measurement. We can see that the measurement results cluster in three "blobs" which are Gaussian distributions, each of which corresponds to ground (g), first-excited (e), and second-excited (f) states. We use this histogram to divide the IQ plane into three "decision regions", shown in Figure 3. Once we've determined these regions, we classify each subsequent measurement as being either e, g, or f by the region it belongs to. Here we define a boolean with 0 as false, 1 as true. We introduce thresholds represented as dashed lines, with g_{bound} being the threshold between the ground and excited state, and e_{bound} being the threshold between the excited and f state.



Figure 3: Qubit readout IQ plane with decision regions plotted.

Qubit Initialization Implementation

Let's first discuss the basic idea of active reset by showing the simplest example of an active reset protocol. We start with a measurement of our qubit, and if the result points to the excited state, we play a pi pulse. This is a very simple protocol, as can be seen in the code block below; we just need to include one threshold bound which differentiates between the ground and excited state (here dubbed g_{bound}). While this method is very fast, it typically does not allow us to reach very high fidelities due to measurement errors, discrimination errors, and pi pulse errors. That's why we need to go a step further, which is the goal of this demonstration.

```

1 | measure('meas_op_res', 'res', None, \
2 |     q demod full('integ_w_s', 0))
3 |
4 | With if_(Q > g_bound):
5 |     play('pi', 'qubit')

```

Now, let's discuss the wait-until-success active reset scheme we propose. First, we introduce the code, which looks like this, with g_{bound} being the ground state threshold and e_{bound} being the excited state threshold.

We will introduce the following time variables (these times are general, and are all quite conservative and can be reduced to decrease run-time):

- $waitTime$: minimal wait time between readout, around 1 us.
- $buffer$: buffer added in case the user has measured something earlier; 10 us as a buffer.
- T_{J} : lifetime of cavity with some buffer (for example, lifetime $x 6 = 6.4$ us)
- $Integ_w_c/integ_w_s$: demodulation weights

```

1 | def initialize(I, 0, g_bound, e_bound, waitTime):
2 |     wait(buffer)
3 |     measure('meas_op_res', 'res', None, \
4 |             q demod full('integ_w_c', I), \
5 |             q demod full('integ_w_s', 0))
6 |
7 |     with while_(Q > g_bound):
8 |         wait(waitTime, 'res')
9 |         align(resonator, 'qubit')
10 |         play('pi01', 'drive01')

```

Now let's break it down a little. The idea in this code is that we want to constantly assess if we're in the ground, excited, or f state (f being any higher-order state). We look at the outputs we get from our qubit, namely the I and Q values (in-phase and quadrature components) [1]. We know which values correspond to the Gaussian distribution of the various states we're examining. We place two bounds in the IQ plane. The first one, g_{bound} , distinguishes between the g state and all other states. We place this bound close to the g Gaussian peak. As we lower the value of the bound, we will classify fewer and fewer points as ground – only those for which we have more certainty. Thus, we can use this parameter to control the fidelity of the initialization scheme – as we decrease it, we will increase the fidelity but spend more time in the initialization scheme. This is a general property of initialization schemes.

If $Q < g_{\text{bound}}$, we classify the measurement as being definitely in the ground state. Otherwise, we assume we're in the excited state and thus play a pi pulse to get to the ground state. We then check if we're in the f state by checking whether or not we've passed e_{bound} (the bound between the excited and f state). If so, we apply a pi pulse between the e and f states and try again. There's a chance it's now in the ground state, so we check if that is the case by running the loop again. If not, we will be in the excited state and thus apply another pi pulse. We loop over this until we're sure the qubit is in the ground state.

Something that we must recognize here is that the QPXP+ and QUA give us the flexibility to perform complex decision sequences and state machine implementations that take into account higher excited states. This can be seen in Figure 4. There is no hardcoded logic or specific assumptions made in the design of the QPXP+ to enable this sequence, and many sequences such as this one can be created by you, limited only by your imagination! (And feedback latency, which is approximately 200 ns for the QPXP+).

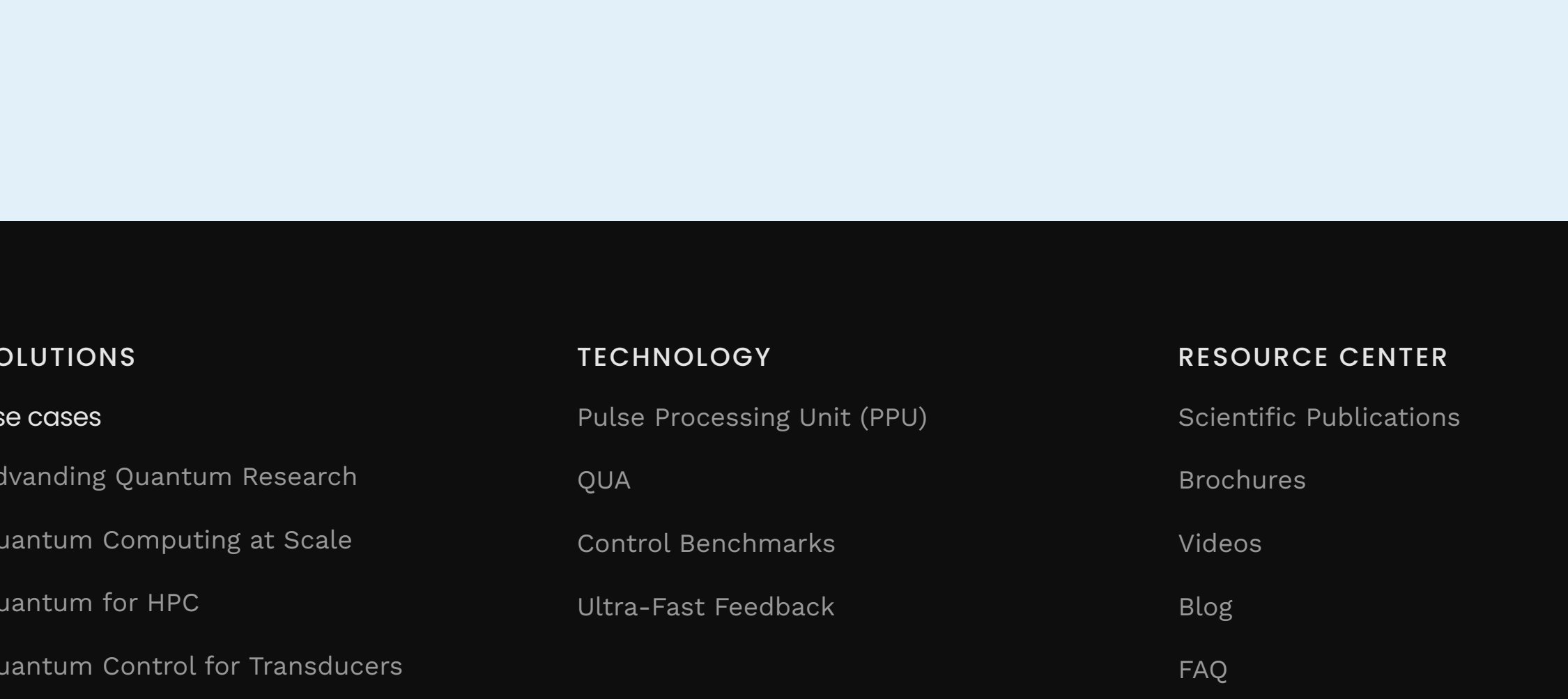


Figure 4: State machine for qubit initialization scheme. See the explanation in the main text.

Active Reset Results

We know show you this protocol at which we propose. Here, we run to show, and we can sum up what's better this works. However, Figure 5 shows the success probability using a confusion matrix. The x-axis displays the measured states, while the y-axis displays the predicted states. To have the highest success, we perform an active reset sequence, then prepare a state to be the immediate for measurement (g, e, and f) state. Thus, we have the highest probabilities on the diagonals of the confusion matrix. For clarity, the measurement without active reset is 4.7% probability, while with the reset, it drops to 0.4%.

Figure 5: Confusion matrix showing the measured and prepared state results with and without active reset.

We hope we've convinced you about our earlier claim that active reset improves the probability that the qubit is indeed in the ground state after the initialization. Next, let's discuss the claim that this active reset protocol reduces the qubit initialization time. We do this by running the various experiments next on the qubit and measuring the run times. This was done in collaboration with Q-CTRL, which provided the *Boulder Opal* and *Q-CTRL's closed-loop SU(3)*. The results can be seen in Figure 6. This is not a minor improvement in time.

Figure 6: A bar chart showing the runtime for various qubit operations and their preparation times on LNL hardware. The chart compares 'WITHOUT ACTIVE RESET' and 'WITH ACTIVE RESET' for Rabi, Open(2)-loop, Closed(2)-loop, and Closed(3)-loop operations. The x-axis shows the operation type, and the y-axis shows the runtime in minutes on a logarithmic scale. The 'WITH ACTIVE RESET' bars are consistently shorter than the 'WITHOUT ACTIVE RESET' bars.

Figure 6: A bar chart showing the runtime for various qubit operations and their preparation times on LNL hardware. The chart compares 'WITHOUT ACTIVE RESET' and 'WITH ACTIVE RESET' for Rabi, Open(2)-loop, Closed(2)-loop, and Closed(3)-loop operations. The x-axis shows the operation type, and the y-axis shows the runtime in minutes on a logarithmic scale. The 'WITH ACTIVE RESET' bars are consistently shorter than the 'WITHOUT ACTIVE RESET' bars.

Figure 6: A bar chart showing the runtime for various qubit operations and their preparation times on LNL hardware. The chart compares 'WITHOUT ACTIVE RESET' and 'WITH ACTIVE RESET' for Rabi, Open(2)-loop, Closed(2)-loop, and Closed(3)-loop operations. The x-axis shows the operation type, and the y-axis shows the runtime in minutes on a logarithmic scale. The 'WITH ACTIVE RESET' bars are consistently shorter than the 'WITHOUT ACTIVE RESET' bars.

Figure 6: A bar chart showing the runtime for various qubit operations and their preparation times on LNL hardware. The chart compares 'WITHOUT ACTIVE RESET' and 'WITH ACTIVE RESET' for Rabi, Open(2)-loop, Closed(2)-loop, and Closed(3)-loop operations. The x-axis shows the operation type, and the y-axis shows the runtime in minutes on a logarithmic scale. The 'WITH ACTIVE RESET' bars are consistently shorter than the 'WITHOUT ACTIVE RESET' bars.

Figure 6: A bar chart showing the runtime for various qubit operations and their preparation times on LNL hardware. The chart compares 'WITHOUT ACTIVE RESET' and 'WITH ACTIVE RESET' for Rabi, Open(2)-loop, Closed(2)-loop, and Closed(3)-loop operations. The x-axis shows the operation type, and the y-axis shows the runtime in minutes on a logarithmic scale. The 'WITH ACTIVE RESET' bars are consistently shorter than the 'WITHOUT ACTIVE RESET' bars.

Figure 6: A bar chart showing the runtime for various qubit operations and their preparation times on LNL hardware. The chart compares 'WITHOUT ACTIVE RESET' and 'WITH ACTIVE RESET' for Rabi, Open(2)-loop, Closed(2)-loop, and Closed(3)-loop operations. The x-axis shows the operation type, and the y-axis shows the runtime in minutes on a logarithmic scale. The 'WITH ACTIVE RESET' bars are consistently shorter than the 'WITHOUT ACTIVE RESET' bars.

Figure 6: A bar chart showing the runtime for various qubit operations and their preparation times on LNL hardware. The chart compares 'WITHOUT ACTIVE RESET' and 'WITH ACTIVE RESET' for Rabi, Open(2)-loop, Closed(2)-loop, and Closed(3)-loop operations. The x-axis shows the operation type, and the y-axis shows the runtime in minutes on a logarithmic scale. The 'WITH ACTIVE RESET' bars are consistently shorter than the 'WITHOUT ACTIVE RESET' bars.

Figure 6: A bar chart showing the runtime for various qubit operations and their preparation times on LNL hardware. The chart compares 'WITHOUT ACTIVE RESET' and 'WITH ACTIVE RESET' for Rabi, Open(2)-loop, Closed(2)-loop, and Closed(3)-loop operations. The x-axis shows the operation type, and the y-axis shows the runtime in minutes on a logarithmic scale. The 'WITH ACTIVE RESET' bars are consistently shorter than the 'WITHOUT ACTIVE RESET' bars.

Figure 6: A bar chart showing the runtime for various qubit operations and their preparation times on LNL hardware. The chart compares 'WITHOUT ACTIVE RESET' and 'WITH ACTIVE RESET' for Rabi, Open(2)-loop, Closed(2)-loop, and Closed(3)-loop operations. The x-axis shows the operation type, and the y-axis shows the runtime in minutes on a logarithmic scale. The 'WITH ACTIVE RESET' bars are consistently shorter than the 'WITHOUT ACTIVE RESET' bars.

Figure 6: A bar chart showing the runtime for various qubit operations and their preparation times on LNL hardware. The chart compares 'WITHOUT ACTIVE RESET' and 'WITH ACTIVE RESET' for Rabi, Open(2)-loop, Closed(2)-loop, and Closed(3)-loop operations. The x-axis shows the operation type, and the y-axis shows the runtime in minutes on a logarithmic scale. The 'WITH ACTIVE RESET' bars are consistently shorter than the 'WITHOUT ACTIVE RESET' bars.

Figure 6: A bar chart showing the runtime for various qubit operations and their preparation times on LNL hardware. The chart compares 'WITHOUT ACTIVE RESET' and 'WITH ACTIVE RESET' for Rabi, Open(2)-loop, Closed(2)-loop, and Closed(3)-loop operations. The x-axis shows the operation type, and the y-axis shows the runtime in minutes on a logarithmic scale. The 'WITH ACTIVE RESET' bars are consistently shorter than the 'WITHOUT ACTIVE RESET' bars.

Figure 6: A bar chart showing the runtime for various qubit operations and their preparation times on LNL hardware. The chart compares 'WITHOUT ACTIVE RESET' and 'WITH ACTIVE RESET' for Rabi, Open(2)-loop, Closed(2)-loop, and Closed(3)-loop operations. The x-axis shows the operation type, and the y-axis shows the runtime in minutes on a logarithmic scale. The 'WITH ACTIVE RESET' bars are consistently shorter than the 'WITHOUT ACTIVE RESET' bars.

Figure 6: A bar chart showing the runtime for various qubit operations and their preparation times on LNL hardware. The chart compares 'WITHOUT ACTIVE RESET' and 'WITH ACTIVE RESET' for Rabi, Open(2)-loop, Closed(2)-loop, and Closed(3)-loop operations. The x-axis shows the operation type, and the y-axis shows the runtime in minutes on a logarithmic scale. The 'WITH ACTIVE RESET' bars are consistently shorter than the 'WITHOUT ACTIVE RESET' bars.

Figure 6: A bar chart showing the runtime for various qubit operations and their preparation times on LNL hardware. The chart compares 'WITHOUT ACTIVE RESET' and 'WITH ACTIVE RESET' for Rabi, Open(2)-loop, Closed(2)-loop, and Closed(3)-loop operations. The x-axis shows the operation type, and the y-axis shows the runtime in minutes on a logarithmic scale. The 'WITH ACTIVE RESET' bars are consistently shorter than the 'WITHOUT ACTIVE RESET' bars.

Figure 6: A bar chart showing the runtime for various qubit operations and their preparation times on LNL hardware. The chart compares 'WITHOUT ACTIVE RESET' and 'WITH ACTIVE RESET' for Rabi, Open(2)-loop, Closed(2)-loop, and Closed(3)-loop operations. The x-axis shows the operation type, and the y-axis shows the runtime in minutes on a logarithmic scale. The 'WITH ACTIVE RESET' bars are consistently shorter than the 'WITHOUT ACTIVE RESET' bars.

Figure 6: A bar chart showing the runtime for various qubit operations and their preparation times on LNL hardware. The chart compares 'WITHOUT ACTIVE RESET' and 'WITH ACTIVE RESET' for Rabi, Open(2)-loop, Closed(2)-loop, and Closed(3)-loop operations. The x-axis shows the operation type, and the y-axis shows the runtime in minutes on a logarithmic scale. The 'WITH ACTIVE RESET' bars are consistently shorter than the 'WITHOUT ACTIVE RESET' bars.

Figure 6: A bar chart showing the runtime for various qubit operations and their preparation times on LNL hardware. The chart compares 'WITHOUT ACTIVE RESET' and 'WITH ACTIVE RESET' for Rabi, Open(2)-loop, Closed(2)-loop, and Closed(3)-loop operations. The x-axis shows the operation type, and the y-axis shows the runtime in minutes on a logarithmic scale. The 'WITH ACTIVE RESET' bars are consistently shorter than the 'WITHOUT ACTIVE RESET' bars.

Figure 6: A bar chart showing the runtime for various qubit operations and their preparation times on LNL hardware. The chart compares 'WITHOUT ACTIVE RESET' and 'WITH ACTIVE RESET' for Rabi, Open(2)-loop, Closed(2)-loop, and Closed(3)-loop operations. The x-axis shows the operation type, and the y-axis shows the runtime in minutes on a logarithmic scale. The 'WITH ACTIVE RESET' bars are consistently shorter than the 'WITHOUT ACTIVE RESET' bars.

Figure 6: A bar chart showing the runtime for various qubit operations and their preparation times on LNL hardware. The chart compares 'WITHOUT ACTIVE RESET' and 'WITH ACTIVE RESET' for Rabi, Open(2)-loop, Closed(2)-loop, and Closed(3)-loop operations. The x-axis shows the operation type, and the y-axis shows the runtime in minutes on a logarithmic scale. The 'WITH ACTIVE RESET' bars are consistently shorter than the 'WITHOUT ACTIVE RESET' bars.

Figure 6: A bar chart showing the runtime for various qubit operations and their preparation times on LNL hardware. The chart compares 'WITHOUT ACTIVE RESET' and 'WITH ACTIVE RESET' for Rabi, Open(2)-loop, Closed(2)-loop, and Closed(3)-loop operations. The x-axis shows the operation type, and the y-axis shows the runtime in minutes on a logarithmic scale. The 'WITH ACTIVE RESET' bars are consistently shorter than the 'WITHOUT ACTIVE RESET' bars.

Figure 6: A bar chart showing the runtime for various qubit operations and their preparation times on LNL hardware. The chart compares 'WITHOUT ACTIVE RESET' and 'WITH ACTIVE RESET' for Rabi, Open(2)-loop, Closed(2)-loop, and Closed(3)-loop operations. The x-axis shows the operation type, and the y-axis shows the runtime in minutes on a logarithmic scale. The 'WITH ACTIVE RESET' bars are consistently shorter than the 'WITHOUT ACTIVE RESET' bars.

Figure 6: A bar chart showing the runtime for various qubit operations and their preparation times on LNL hardware. The chart compares 'WITHOUT ACTIVE RESET' and 'WITH ACTIVE RESET' for Rabi, Open(2)-loop, Closed(2)-loop, and Closed(3)-loop operations. The x-axis shows the operation type, and the y-axis shows the runtime in minutes on a logarithmic scale. The 'WITH ACTIVE RESET' bars are consistently shorter than the 'WITHOUT ACTIVE RESET' bars.

Figure 6: A bar chart showing the runtime for various qubit operations and their preparation times on LNL hardware. The chart compares 'WITHOUT ACTIVE RESET' and 'WITH ACTIVE RESET' for Rabi, Open(2)-loop, Closed(2)-loop, and Closed(3)-loop operations. The x-axis shows the operation type, and the y-axis shows the runtime in minutes on a logarithmic scale. The 'WITH ACTIVE RESET' bars are consistently shorter than the 'WITHOUT ACTIVE RESET' bars.

Figure 6: A bar chart showing the runtime for various qubit operations and their preparation times on LNL hardware. The chart compares 'WITHOUT ACTIVE RESET' and 'WITH ACTIVE RESET' for Rabi, Open(2)-loop, Closed(2)-loop, and Closed(3)-loop operations. The x-axis shows the operation type, and the y-axis shows the runtime in minutes on a logarithmic scale. The 'WITH ACTIVE RESET' bars are consistently shorter than the 'WITHOUT ACTIVE RESET' bars.

Figure 6: A bar chart showing the runtime for various qubit operations and their preparation times on LNL hardware. The chart compares 'WITHOUT ACTIVE RESET' and 'WITH ACTIVE RESET' for Rabi, Open(2)-loop, Closed(2)-loop, and Closed(3)-loop operations. The x-axis shows the operation type, and the y-axis shows the runtime in minutes on a logarithmic scale. The 'WITH ACTIVE RESET' bars are consistently shorter than the 'WITHOUT ACTIVE RESET' bars.

Figure 6: A bar chart showing the runtime for various qubit operations and their preparation times on LNL hardware. The chart compares 'WITHOUT ACTIVE RESET' and 'WITH ACTIVE RESET' for Rabi, Open(2)-loop, Closed(2)-loop, and Closed(3)-loop operations. The x-axis shows the operation type, and the y-axis shows the runtime in minutes on a logarithmic scale. The 'WITH ACTIVE RESET' bars are consistently shorter than the 'WITHOUT ACTIVE RESET' bars.

<p